JOURNAL OF APPLIED ELECTROCHEMISTRY 14 (1984) 315–322

Hydrogen insertion (intercalation) and light induced proton exchange at TiO_2(B)-electrodes

G. BETZ, H. TRIBUTSCH

Hahn-Meitner-Institut für Kernforschung Berlin, Bereich Strahlenchemie, Postbox D-1000, Berlin 39, Federal Republic of Germany

R. MARCHAND

Laboratoire de Chimie des Solides associé au CNRS (LA 279), 2 rue de la Houssinière, F-44072 Nantes-Cedex, France

Received 16 June 1983; revised 11 July 1983

TiO_2(B) obtained from $K_2Ti_4O_9$ by hydrolysis and subsequent heating is a semiconductor whose crystal structure allows the insertion of guest atoms. Photoelectrochemical experiments characterized the polycrystalline material as n-type with an energy gap of 3 eV. As a result of electrochemical reduction of protons at TiO_2(B)-electrodes new electronic states appear within the energy gap, making the semiconductor sensitive for visible light. These states originate from intercalated hydrogen which diffuses through the sample. Upon optical excitation of these states an anodic photocurrent is observed that can be interpreted as light-induced deintercalation of hydrogen from TiO_2(B) to give protons.

1. Introduction

It is well-known that nature has evolved energy transducing membranes in which solar energy is used to pump protons for the purpose of electrochemical energy storage. The purple membrane of halobacterium halobium as well as the photosynthetic membrane of green plants are examples of this mechanism which is actually explained by the framework of the chemiosmotic hypothesis (Mitchell) [1, 2].

Model systems aimed at reproducing such light-driven proton pumps have already been discussed [3]. A reasonable way to transfer ions across an interface between liquid and condensed matter with the help of light energy would seem to be light-induced intercalation/deintercalation of semiconducting host materials. This mechanism is based on the fact that intercalation and deintercalation of many electrode materials can be performed by electrochemical reduction and oxidation, respectively [4]. Since many host materials suitable for intercalation are semiconductors (e.g. ZrS_2, $ZrSe_2$, HfS_2, $HfSe_2$, MoS_2, WS_2, $FePS_3$ and $MoSe_2$), the ion transfer mechanism can in principle be stimulated by light. The most attractive electrolyte for the intercalation and deintercalation of protons is water. Unfortunately, aqueous electrolytes are little suited to ion exchange with the above mentioned host materials. One reason is the co-intercalation of water products which makes intercalation partially irreversible and leads to corrosion. Another reason is the danger of partially reducing the host electrodes with formation of H_2S and H_2Se, respectively [5].

During the search for new materials with which these difficulties can be avoided, it was concluded that the new modification of TiO_2, named TiO_2(B), might be suitable for this purpose. TiO_2 (rutile) has been extensively studied as a semiconductor for photoelectrolysis of water. It proved to be a reasonably stable material [6–8].

Several authors have reported the electrochemical charging and discharging of TiO_2 (rutile) with hydrogen [9–13]. ESR-measurements, capacity measurements and electrochemical kinetic experiments have been presented in support of models on a hydrogen bronze of TiO_2 [14]. Electron stimulated desorption measurments show that electrochemical doping with hydrogen

0021–891X/84 $03.00 + .12

occurs in a layer of approximately 100 μm at the electrode surface [15]. Both hydrogen on interstitial sites and the protonic form have been proposed to exist in TiO_2 (rutile) [13]. Incorporation of hydrogen into TiO_2 (rutile) turns the colour of the sample into a characteristic blue [11]. The colour change, however, does not mean that the spectral dependence of photocurrents at TiO_2 (rutile) shifts into the visible region, since the change of colour is caused by free carrier absorption. A sensitivity change of the UV-photocurrents has, however, been reported.

An attempt was made to induce these reactions with light at TiO_2(B)-electrodes. This perovskite-related modification of TiO_2 was investigated and was found to provide cavities and channels which considerably improve the conditions for insertion and transport of hydrogen or other small cations [16].

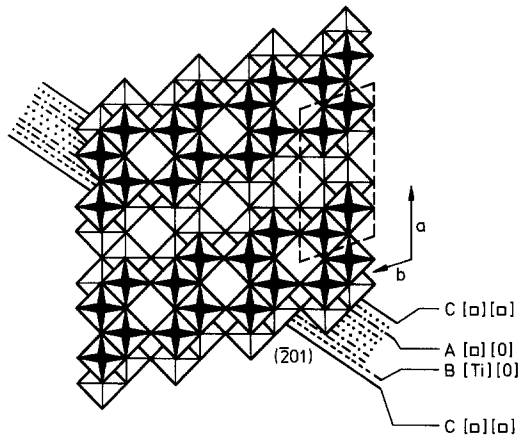

Fig. 1. Projection of the idealized structure of TiO_2(B) along [010]. The structure can be regarded as composed of planes A, B, C in a sequence $[(BAAB)_2C]_n$. Plane A contains oxygen ions and titanium vacancies; plane B contains oxygen and titanium ions and plane C consists of oxygen and titanium vacancies [19].

2. Experimental details

2.1. *Material*

TiO_2(B), a white compound, had been prepared by hydrolysis of $K_2Ti_4O_9$ followed by filtration and thermolysis. TiO_2(B) has a perovskite-related structure [17]. Perovskite-type structures characteristically contain cubo-octahedron cavities which are often occupied by cations such as Cu^{2+}, Ba^{2+} and Na^+ or Li^+. This cavity is vacant in a number of compounds typified by ReO_3 [18]. TiO_2(B) can be considered as a material which is built up of ReO_3-type units. The idealized three-dimensional framework of TiO_2(B) is shown in Fig. 1.

2.2. *Sample preparation*

Electrodes were made by pressing TiO_2(B)-powder at room temperature into discs of diameter 4 mm and of thickness 0.5 mm. The pressure at this temperature was below the value at which the TiO_2(B)-modification changes into anatase [18]. At 400° C the pressed samples were sintered in an evacuated glass tube (4×10^{-5} mb) for 48 h. Fig. 2 shows the polycrystalline structure of the samples produced by this method. From the sign of the Seebeck coefficient measured with a hot probe (GCA, Solid State Measurements) the material was identified as n-type.

Ohmic back contact was made by an indium–mercury alloy. The samples were fixed with silver paste (3M) on to an electrode holder of brass. For the experiments the electrode surface was left in its native state without polishing or etching to avoid damage of the sintered microcrystalline structure. The sides of the disc and the brass centre of the electrode holder were electrically isolated with epoxy resin (3M Scotchcast).

The experimental set-up shown in Fig. 3 consisted of two compartments separated by a PVC plate. A TiO_2(B)-sample was put onto a hole in the

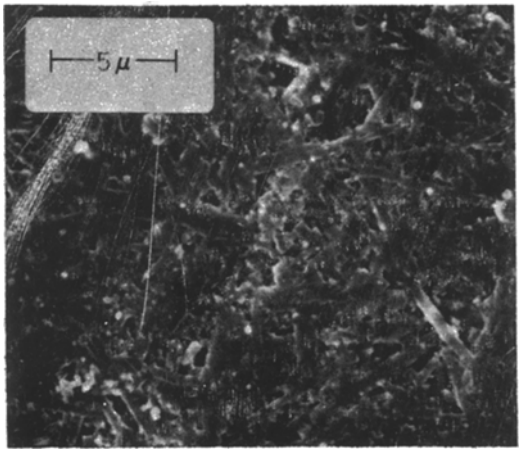

Fig. 2. SEM-photo of a pressed and sintered TiO_2(B)-electrode.

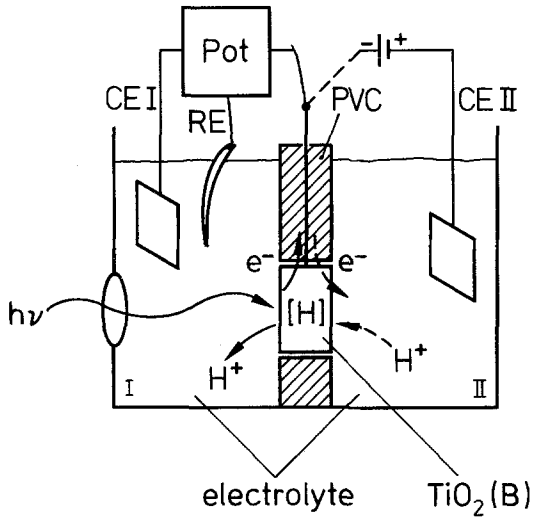

Fig. 3. Two compartment electrochemical set-up. Both compartments are separated with a PVC plate. The TiO_2(B) electrode is mounted onto a hole in the centre of the plate.

centre of the PVC plate and electrically contacted. This was achieved in the following way: the TiO_2(B)-sample was glued with silver epoxy onto a ring of silver foil. A silver wire was welded onto the foil which was then glued onto the PVC plate and electrically isolated with epoxy resin leaving only the front and back surface of the TiO_2(B)-electrode free for contact with the electrolytes.

With an aqueous solution of 0.1 mol dm^{-3} K_2SO_4 the electrical resistance between the two cells measured with a platinum electrode was that of the TiO_2(B)-electrode itself, which showed the absence of an electrolytic contact between the cells. A further test for the absence of an electrolytic leak was made by filling one cell with a saturated K_2SO_4 solution and the other with concentrated $BaCl_2$ solution. After several hours no $BaSO_4$ was found in either compartment.

Thus the only way electronic and ionic current as well as elements (e.g. H) could pass from one cell to the other was through the TiO_2(B)-electrode.

2.3. *Experimental set up*

Photoelectrochemical experiments were performed in a standard three electrode cell with a Pt-electrode as counter and a Hg_2SO_4-electrode (Metrohm) as a reference electrode. The experiments were performed in an aqueous 0.1 mol dm^{-3} H_2SO_4 solution or in an 0.1 mol dm^{-3} tetraethylammoniumperchlorate (TEAPC) solution. In the H_2SO_4 solution the pH was adjusted by adding H_2SO_4 or KOH.

Cyclic voltammograms were obtained with a potentiostat (Bank POS 73). As light sources either a 450 W Xe lamp (Oriel) or an argon ion laser (Model 165 Spectraphysics, $\lambda = 514.5$ nm) were used. Photocurrent spectra were obtained with a high-intensity monochromator (Bausch and Lomb) equipped with a grating blazed at 700 nm.

3. Results

A typical cyclic voltammogram of a polycrystalline TiO_2(B)-electrode is presented in Fig. 4 which shows a marked hysteresis. This corresponds to the time dependence of both anodic and cathodic dark currents. At a constant negative potential cathodic dark currents gradually decrease with time.

If the potential of the electrode is then fixed at a more positive value, an anodic discharge current starts to flow which also decreases with time. The

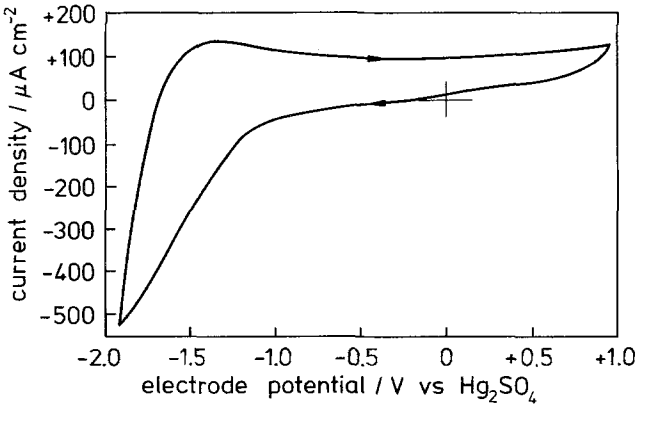

Fig.4 Cyclic voltammogram of a TiO_2(B)-electrode in a 0.1 mol dm^{-3} K_2SO_4 (aq) solution. The scan rate was 20 mV s^{-1}.

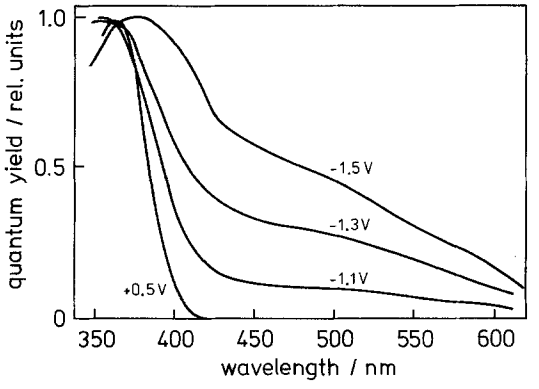

Fig. 5. Spectral dependence of photocurrents for different applied electrode potentials are measured against a Hg_2SO_4 reference electrode. At each potential the electrode was allowed to reach equilibrium. Each of the spectra is normalized.

TiO_2(B)-electrode proved to be stable during many cycles so that the observed currents cannot be due to corrosion. Since potassium could be excluded as a possible reactant through the replacement of H_2SO_4 by TEAPC only hydrogen interacting with TiO_2(B) needs to be considered as the cause for the pronounced hysteresis. This is also confirmed by the pH-dependence of the onset of the cathodic dark currents, which attributes these currents to proton reduction.

The photoelectrochemical behaviour of TiO_2(B) proved to be relatively complex; the following experiments however suggest that it arises essentially from two fundamentally different contributions:

(a) a photocurrent generated as a consequence of absorption of UV-light in the bulk of TiO_2(B) and

(b) a photocurrent which arises after hydrogen has been intercalated into the electrode and which could also be generated by visible light.

One evidence for the participation of two different photoelectrochemical mechanisms is the pronounced variation of the spectral dependence of photocurrents with the applied electrode potential (Fig. 5). When a positive potential (+ 0.5 V vs Hg_2SO_4) is applied to the TiO_2(B)-electrode in the equilibrium situation photocurrents can be excited only with UV-light. From the position of the absorption edge an energy gap of approximately 3.0 eV can be deduced. The occurrence of anodic currents is well in agreement with the n-type character of the material determined with Seebeck-effect measurements. Since no corrosion became evident through prolonged operation (3×10^3 Coulomb), it was concluded that the photocurrent involved the oxidation of water as in the case of TiO_2 (rutile).

When a negative potential ($E_g = -1.5$ V vs Hg_2SO_4) is applied to the TiO_2(B)-electrode another kind of anodic photocurrent is observed. It starts at small values and gradually increases with time until it reaches a saturation value (Fig. 6a). In a steady state situation the spectral distribution of this photocurrent is considerably shifted towards longer wavelengths (Fig. 5). A relation of this photoresponse to the insertion of hydrogen as a consequence of proton reduction is not only indicated by the potential range in which it occurs but also by a simultaneous decrease of the cathodic dark current, which is characteristic for intercalation mechanisms in which transport becomes a limiting factor.

A TiO_2(B)-electrode previously charged in the negative potential region retains its altered spectral sensitivity for some time after changing the electrode potential to smaller values, where a discharge of the electrode becomes possible. There is, however, a gradual decay of both anodic dark current and anodic photocurrent (Fig. 6b). That portion of the photocurrent spectrum that finally remains can be excited only by UV-light.

Fig. 5 shows that in an equilibrium situation the spectral sensitivity changes gradually with the electrode potential as long as a cathodic dark current is flowing. This change of the spectral response of the photocurrent is accompanied by a change in the absorption of the TiO_2(B)-electrode. The colour of the electrode turned from white to blue when the potential was shifted from + 0.5 to − 1.5 V. As a consequence of such a potential displacement, the reflected intensity of 514.5 nm laserlight decreased by 5%. The quasi-stationary photocurrent behaviour (potential steps of 0.1 V with 10 s resting) of TiO_2(B) is shown in Fig. 7 with xenon-light and in Fig. 8 with laser light.

An anodic saturation current is reached at a positive voltage. During sweeping to more negative potential values the anodic photocurrent drops with a pronounced hysteresis (see Fig. 8). In this case the characteristic shape of the photocurrent–voltage curve arises from photoeffects generated

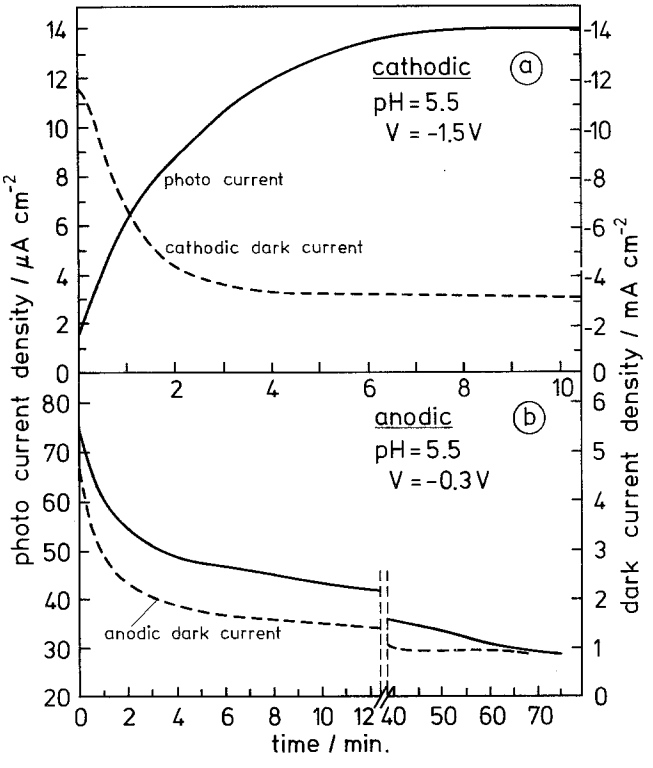

Fig. 6. Time dependence of the photo- and dark-current at a TiO_2(B)-electrode. The potentials are measured against a Hg_2SO_4 reference electrode. In the case of (a) the electrode had been previously equilibrated at a positive potential of 0.5 V; in the case of (b) it had been equilibrated at − 1.5 V.

both by UV and visible light. Part of the UV-photoeffect is due to anodic photo-oxidation of water. The photocurrent induced by visible light is only observed after proton insertion at negative potentials and disappears at more postive potentials. This photocurrent is shown separately in Fig. 8 where 514.5 nm laserlight was used for excitation. In this case the photoresponse is bigger at negative potentials where proton insertion is occurring. The behaviour of TiO_2(B) at two different pH-values has been compared. In a qualitative way the photocurrent shifts parallel to proton reduction.

In order to support the suggestions that electrochemical hydrogen insertion into TiO_2(B) is responsible for the photoeffect in the visible spectral region the set-up of Fig. 3 was used for the following tests. A TiO_2(B)-sample was prepared as an electrode plate of 0.5 mm facing the electrolytes of two independent electrochemical cells (I and II). The idea was to insert hydrogen electrochemically by activating circuit II to allow hydro-

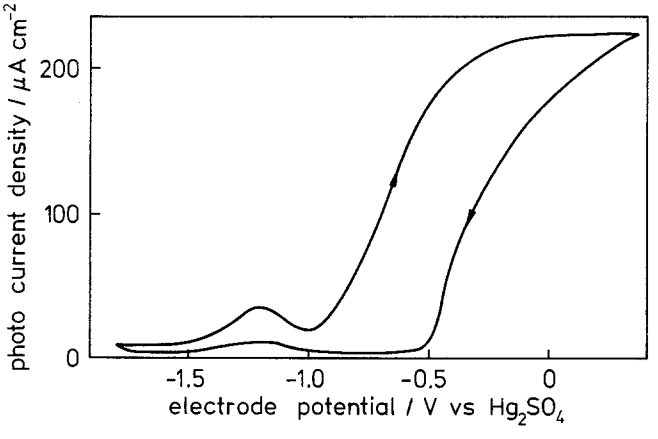

Fig. 7. The dependence of the photocurrent density on the applied electrode potential. The electrode was illuminated with a 450 W Xenon lamp.

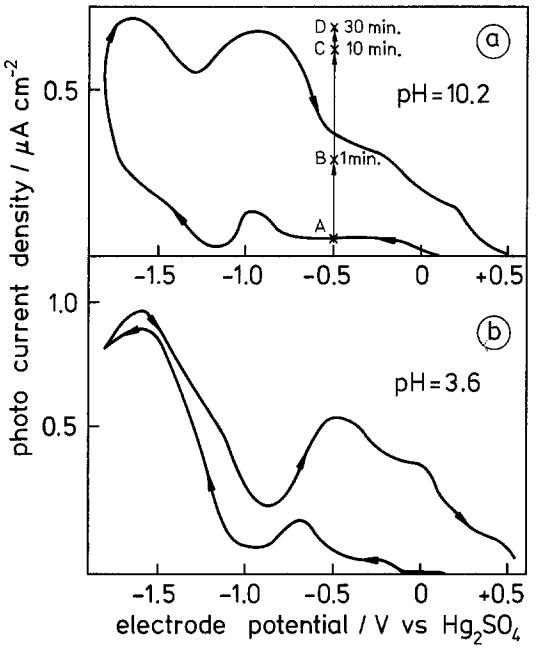

Fig. 8. Photocurrent-voltage curves at an TiO_2(B)-electrode for different pH-values. The TiO_2(B)-electrode was illuminated with laser light ($\lambda = 514.5$ nm, $I = 32.4$ mW cm^{-2}). A, B, C, D show the photocurrent density in cell I of the experimental design of Fig. 3 after having applied -1.8 V versus Hg_2SO_4 at the electrode in cell II for different time intervals.

gen to diffuse to the opposite TiO_2(B)/electrolyte interface and to use the principal circuit I to detect photocurrents generated with visible light. At first a potential of -0.5 V was applied to the electrode surface facing cell II. Under this condition anodic photocurrents excited by visible light (514.5 nm) went close to zero (A in Fig. 8a). Circuit II remained open during this period of conditioning. Then circuit I was switched off and left under open circuit conditions. Subsequently a potential of -1.2 V vs Hg_2SO_4 was applied to the TiO_2(B) surface facing cell II. Circuit I was reactivated and photoeffects measured at -0.5 V vs Hg_2SO_4 with 514.5 nm laserlight. This procedure was repeated for different periods of electrochemical insertion of hydrogen through circuit II. A clear increase of the photoeffects at 514.5 nm was subsequently observed on the opposite sample surface. This increase is indicated in Fig. 8a for hydrogen insertion periods of 1 min, 10 min and 30 min, respectively.

The dependence of photocurrents generated with the laser ($\lambda = 514.5$ nm) light intensity has been measured at different electrode potentials (-1.5 V, -1.4 V, -1.3 V, and -1.0 V vs Hg_2SO_4). They correspond to conditions of different rates of hydrogen intercalation. The results are shown in Fig. 9. A linear behaviour and no saturation is observed at potentials more negative than -1.0 V vs Hg_2SO_4 for lignt intensities up to 1.1 W cm^{-2}. The determination of the flat band potential of TiO_2(B) by capacity measurements has been attempted. The capacitance–voltage curves could not be analysed in terms of a Mott–Schottky plot. One reason may be the large amounts of defects and surface states in the polycrystalline material. There was a pronounced hysteresis in the C–V curves when sweeping the potential from negative to positive values and back. The capacitance increased when the electrode was held at negative potentials. This increase may be due to extra positive ionic charges within the space charge layer arising from ionized hydrogen.

4. Discussion

The experimental evidence presented suggests the coexistence of two different mechanisms of photocurrent generation in TiO_2(B). There is a photoeffect which is due to absorption of UV-photons which are exciting electrons from the valence band to the conduction band of TiO_2(B). This mechanism can at positive potentials induce photooxidation of water and should not be discussed further because of its parallelism to TiO_2 (rutile). The second kind of photoeffect arises as a consequence of electrochemical hydrogen intercalation. It is characterized by the generation of electronic states in the forbidden energy gap of the material, accompanying the diffusion of hydrogen through the electrode. The experiment with a thin TiO_2(B) sample between two separate electrolytes does not seem to permit other interpretations. The reversible generation and suppression of photoeffects in the visible spectral region as well as the fact that additional photoeffects can be generated cannot be explained without assuming such electronic states in the forbidden energy gap. At present a reasonable model for the generation of these states on the basis of a chemical interaction between intercalated hydrogen and TiO_2(B) cannot be provided. The energy scheme of Fig. 10 shows the

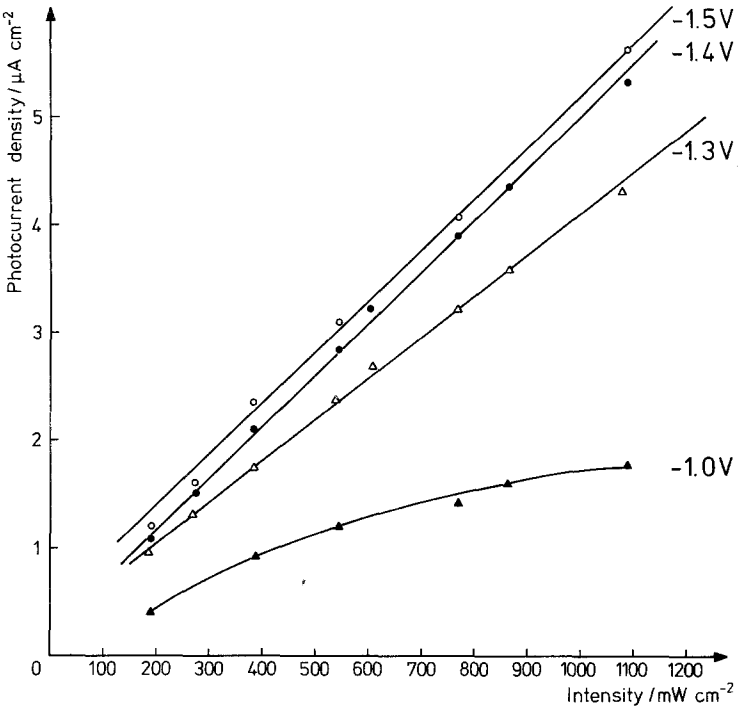

Fig. 9. Dependence of the photocurrent density on the light intensity at a TiO_2(B)-electrode. The potential was measured against a Hg_2SO_4 reference electrode. At each applied potential the electrode was equilibrated. A laser (λ = 514.5 nm) was used as a light source.

two electrolytic interfaces of a thin TiO_2(B)-plate as mounted in the electrochemical set up with two adjacent cells of Fig. 3. Electrochemical intercalation of hydrogen generates intercalation states in the forbidden energy region of the semiconducting host material. These states must be occupied by electrons since the Fermi level is only a little distance below the conduction band. Experimentally it has been confirmed that both the negative and positive potential regions ionization of these states are accompanied by the generation of an anodic photocurrent. As Fig. 10 indicates, this phenomenon can be interpreted in terms of a light-induced deintercalation of hydrogen. Protons separated from their electrons are forced to leave the electrode surface. In the presence of a positive space charge layer (left interface in Fig. 10) such a mechanism can be easily imagined. In the case of a negative space charge layer anodic photocurrents are occurring simultaneously with electrochemical intercalation of hydrogen. Under such conditions a high concentration of intercalation states can be assumed very close to the electrode surface. From these states protons do not have to overcome large potential barriers during their light-induced transfer into the electrolyte.

Our experiments and theoretical considerations suggest the possibility that generation of hole/electron pairs in the energy band of the host material by UV-photons equally triggers the deintercalation of hydrogen to give protons. In

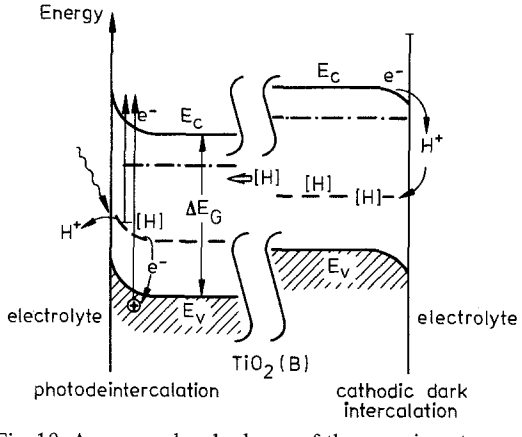

Fig. 10. An energy band scheme of the experiment showed in Fig. 3. Intercalation of hydrogen at the right side of the TiO_2(B)-electrode creates electronic states in the energy gap. Hydrogen atoms move to the left side of the electrode creating there also midgap states. From these states electrons can be excited with visible light into the conduction band of TiO_2(B). The protons are released into the electrolyte. It is also possible that holes created by UV-photons in the valence band trap electrons from the intercalation states which also leads to a deintercalation of hydrogen.

this case electrons on intercalation states would recombine with holes in the valence band of TiO_2(B) in a primary step followed by a release of protons into the electrolyte. The main evidence for such a mechanism is the increase of the photocurrent efficiency towards the UV bulk absorption in the case of a negative electrode potential ($-$ 1.5 V vs Hg_2SO_4).

Since the spectral dependences in Fig. 5 have been normalized, it has to be emphasized that absolute efficiencies at + 0.5 V reach only 5% of the value at $-$ 1.5 V (quantum efficiency $\phi(-1.5\,V) = 3 \times 10^{-2}$, $\phi(+0.5\,V) = 1.4 \times 10^{-3}$). The photoeffect associated with hydrogen deintercalation is thus much more pronounced than the anodic bulk photoeffect of sintered TiO_2(B) up to an electrode potential of + 0.5 V. More experimental studies will be needed to further clarify the origin and mechanism of visible light-photoeffects in TiO_2(B). Several observations are in agreement with the assumption that proton reduction at this material is followed by both an insertion of neutral hydrogen and of protons (with electrons in the conduction band of TiO_2). The first species contributes to the long wavelength deintercalation photocurrent, the second to the deintercalation dark current.

Although it is evident that much more information is needed on photoeffects at semiconductor electrodes associated with intercalation and deintercalation of guest molecules, it already seems to be clear that they deserve further investigations with respect to several possible applications: storage of solar energy in intercalation compounds, the light-induced pumping of ions across membranes, the storage of optical information and electrochromic devices.

Acknowledgement

We would like to thank our colleagues for many valuable discussions.

References

[1] D. Oesterhelt and W. Stockenius, *Proc. Natn. Acad. Sci. USA* **70** (1973) 2853.
[2] P. Mitchell, *J. Bioenergy* 4 (1973) 63.
[3] G. W. Murphy, M. F. Lemons and M. Springer, *Solar Energy* **28** (1981) 403.
[4] H. Tributsch, *Appl. Phys.* **23** (1980) 61.
[5] A. Lerf and R. Schöllhorn, *Inorg. Chem.* **16** (1977) 2950.
[6] A. Fujishima and K. Honda, *Nature* **238** (1972) 37.
[7] A. J. Nozik, *ibid.* **257** (1975) 383.
[8] H. Gerischer in 'Solar Power and Fuels – Proceedings of the First International Conference on the Photochemical Conversion and Storage of Solar Energy' (edited by J. R. Bolton) Academic Press, New York (1977) Ch. 4, p. 106.
[9] D. W. Johnson, S. H. Paek and J. W. Ford, *J. Appl. Phys.* **46** (1975) 1026.
[10] D. Haneman and F. Steenbeck, *J. Electrochem. Soc.* **124** (1977) 861.
[11] D. S. Ginley and M. C. Knotek, *ibid.* **126** (1979) 2163.
[12] R. H. Wilson, L. A. Harris and M. E. Gerstner, *ibid.* **126** (1979) 844.
[13] R. Schuhmacher, *Ber. Bunsenges. Phys. Chem.* 84 (1980) 125.
[14] E. Serwicka, R. N. Schindler and R. Schuhmacher, *ibid.* 85 (1981) 192.
[15] U. L. Knotek and P. J. Ferbelman, *Phys. Rev. Lett.* **40** (1978) 964.
[16] D. W. Murphy and P. A. Christian, *Science* **205** (1979) 651.
[17] R. Marchand, L. Brohan and M. Tournoux, *Mat. Res. Bull.* **15** (1980) 1129.
[18] G. M. Clark, 'The Structure of Non-Molecular Solids' John Wiley, New York (1972) p. 148–50.
[19] L. Brohan, A. Verbaere, M. Tournoux and G. Demazeau, *Mat. Res. Bull.* **17** (1982) 355.